CORROSION SCIENCE AND TECHNOLOGY, Vol.24, No.4(2025), pp.212~229 pISSN 1598-6462 / eISSN 2288-6524
[Research Paper] DOI: https://doi.org/10.14773/cst.2025.24.4.212

Influence of Ethylene Glycol on the Electropolishing of Titanium and the Electrochemical characteristics in PEMFC Environments

Hyun-Kyu Hwang[1] and Seong-Jong Kim[2,†]

[1]*Department of Nuclear and Quantum Engineering, Korea Advanced Institute of Science and Technology, 291 Daehak-ro, Yuseong-gu, Daejeon, 34141, Republic of Korea*
[2]*Division of marine system engineering, Mokpo national maritime university, 91, Haeyangdaehak-ro, Mokpo-si, Jeollanam-do, 58628, Republic of Korea*

(Received July 23, 2025; Revised August 07, 2025; Accepted August 12, 2025)

This research investigated the effects of electropolishing on titanium using choline chloride-based deep eutectic solvents with varying ethylene glycol molar ratios (1:1, 1:2, 1:3) and applied potentials, as well as the electrochemical characteristics in a PEMFC simulated environment. The analysis of the potentiodynamic polarization curves revealed that a choline chloride to ethylene glycol ratio of 1:3 resulted in the most stable current density and the broadest potential range. This stability was attributed to an increased concentration of active ions participating in the electrochemical reaction, which led to the formation of a significant amount of oxygen-bonded metal-organic complexes, thereby stabilizing the dissolution reaction. In titanium (Ti) electropolished under optimal conditions, additional TiO_2 crystalline phases were observed. The investigation of the electrochemical characteristics in the PEMFC simulation solution presented that mechanically polished titanium did not meet U.S. Department of Energy standards, whereas the specimens electropolished under optimal conditions did. This improvement is due to the beneficial influence of the TiO_2 formed during the electropolishing process on the electrochemical characteristics.

Keywords: *Titanium, Eco-friendly electrolyte, Electropolishing, PEMFC, Anti-corrosion*

1. Introduction

Titanium, a transition metal, is widely recognized as a structural material due to its excellent mechanical characteristics and chemical stability [1-3]. Owing to its high specific strength, high melting point (1660 - 1700 ºC), biocompatibility and corrosion resistance, titanium finds extensive applications in the aerospace, automotive, marine and medical fields [4-8]. Notably, titanium exhibits about twice the electrical conductivity of stainless steel, making it a viable candidate for lightweight bipolar plates in proton exchange membrane fuel cells (PEMFCs) [9,10]. According to the International Annealed Copper Standard (IACS), the electrical conductivities of Grade 1 titanium and USN 31603 are approximately 3 – 5% IACS and 2 – 3% IACS, respectively [11]. At this point, IACS is an international standard that defines the electrical conductivity of high-purity copper softened at 20 ºC as 100%. The reason why the electrical conductivity of actual stainless steel is low is that, from an atomic point of view, various alloying elements such as Cr, Ni and Mo cause scattering of free electrons, which reduces the electrical conductivity [12]. On the other hand, high-purity titanium has a low degree of alloying, so electron scattering is relatively low, and it exhibits electrical conductivity that is about 1.5 to 2 times higher than that of stainless steel. However, during PEMFC operation, sulfuric acid and hydrofluoric acid can leach into the electrolyte, degrading the performance of the bipolar plates and reducing their lifespan [13,14]. Coating technology for this is being investigated, and surface treatment such as surface flattening, removal of surface defects and impurities before coating is considered an important technology for improving the performance and lifespan of the bipolar plates [15-17]. Nevertheless, surface treatment of bipolar plates with complex geometries remains challenging [15-17]. Moreover, surface treatment is crucial in high-value-added industries such as pharmaceuticals, semiconductors, cardiovascular·orthopedic implants, coronary stents and surgical instruments [18].

Among various surface treatments, electropolishing

†Corresponding author: ksj@mmu.ac.kr
Hyun-Kyu Hwang: Researcher, Seong-Jong Kim: Professor

offers numerous advantages, including the ability to process complex shapes, enhance corrosion resistance, achieve a mirror finish, clean the surface, relieve surface stress, reduce deformation and inhibit bacterial growth [19].

However, the electrolyte for electropolishing generally uses a strong acid solution such as phosphoric acid, sulfuric acid and perchloric acid-acetic acid solution. However, due to environmental and safety concerns, research is being conducted on using eco-friendly electrolytes [5,20-22].

N. C. Ferreri *et al.* conducted electropolishing using an eco-friendly electrolyte composed of ethanol, ethylene glycol and NaCl for mirror polishing titanium for metallographic analysis [5]. Their results indicated that mechanical polishing was slow due to the strong galling tendency of titanium, and it was challenging because it required the use of abrasives (SiC) and polishing fluids (alumina, diamond). In contrast, electropolishing was relatively fast and simple, producing a clean surface suitable for metallographic analysis. W. O. Karim *et al.* investigated the effect of ethanol on electropolishing in an eco-friendly electrolyte composed of ethanol, ethylene glycol and NaCl [22]. Their study revealed that conventional electropolishing of titanium led to the formation of a titanium dioxide (TiO_2) layer, enhancing corrosion resistance, but this TiO_2 layer was removed in the presence of ethanol in the electrolyte.

However, in the electrolyte mixture of ethylene glycol, ethanol and NaCl, the high volatility of ethanol caused instability in electrolyte concentration, adversely affecting the electropolishing process and making it difficult to apply in real-working environments [23]. Furthermore, NaCl-based electrolytes exhibited relatively low ionic conductivity, resulting in reduced electropolishing efficiency, with approximately one hour of processing time required to achieve a high-quality surface [5,21,23]. Due to these limitations, for stainless steel, electropolishing often employs an eco-friendly electrolyte based on deep eutectic solvents, which are mixtures of salts and hydrogen bond donors [24,25]. Deep eutectic solvents have low volatility and excellent thermal stability, allowing for consistent concentration maintenance. Additionally, they contain high concentrations of ions, resulting in high electrical conductivity, enabling faster and more efficient electropolishing processes.

However, investigations on eco-friendly electropolishing using deep eutectic solvents for titanium are scarce [26]. In particular, research on the application of electropolishing prior to coating for improving PEMFC lifespan is even harder to find [27].

Therefore, this investigation examined the electropolishing effects using choline chloride-based deep eutectic solvents with varying ethylene glycol molar ratios (1:1, 1:2, 1:3) and applied potentials. Additionally, the electrochemical characteristics and damage mechanisms in a PEMFC simulated environment were analyzed.

2. Experimental Methods

2.1 Specimen Preparation

Grade 1 titanium, known for its high purity, was used as the substrate for PEMFC bipolar plates, with the chemical composition shown in Table 1. Grade 1 titanium was chosen for its lower impurity content, superior corrosion resistance, electrical conductivity and high formability, making it suitable for designing flow channels in thin substrates [28,29]. The specimens were processed using a fine-cutter with coolant supply to minimize thermal deformation during machining. The specimens were machined to an exposed area of 4 cm^2 and mounted with epoxy resin. The mounted specimens were mechanically polished up to #600 grit emery paper. Contaminants generated during the polishing process were removed by degreasing with acetone followed by ultrasonic cleaning with distilled water. The specimens were then dried in an oven for approximately one day before being used as working electrodes.

2.2 Electropolishing

2.2.1 Electrolyte Composition

For electropolishing, the eco-friendly electrolyte used

Table 1. Chemical compositions of grade.1 titanium (wt%)

Fe	C	N	H	O	Ti
≤ 0.20	≤ 0.08	≤ 0.03	≤ 0.015	≤ 0.18	Bal

was a type of deep eutectic solvent known as ethaline. Ethaline is a mixture of choline chloride and ethylene glycol ($C_2H_6O_2$). Deep eutectic solvents include reline (ChCl:Urea), glyceline (ChCl:Glycerol) and ethaline (ChCl:Ethylene Glycol). Ethaline has excellent structural and thermal stability, and can induce a dissolution reaction that is effective in forming a uniform oxide film and flattening the surface of titanium. Additionally, Ethaline is effective in electropolishing processes due to its low viscosity and high ionic conductivity compared to other types of deep eutectic solvents. According to the research results of Kityk *et al.* [30], among various types of deep eutectic solvents, ethaline presented the best surface planarization effect during electropolishing. In addition, the electrochemical impedance spectroscopy analysis results presented that the semicircle of the Nyquist plot was largest in the electropolishing specimen using ethaline, indicating the formation of a stable passive film. Based on these research results, ethaline was selected in this investigation. Table 2 presents the molar ratios of choline chloride to ethylene glycol used in this investigation. The electropolishing solution was mixed at 70 °C for 1 hour until it became completely colorless.

2.2.2 Electrochemical Experiments

The electrochemical experiments were conducted using a Gamry Reference 3000 system, with an Ag/AgCl electrode as the reference electrode and a platinum mesh electrode as the counter electrode. Since electropolishing should be performed in the potential range where passivation occurs, potentiodynamic polarization experiments were conducted in the ethaline solution [31]. The potentiodynamic polarization experiments were stabilized at 35 °C for 30 minutes before applying potentials ranging from 0 V to 25 V versus open circuit potential. Electropolishing was then performed at various potentials within the passivation range identified in the potentiodynamic polarization curves. The electropolishing process is a technique that applies high voltage, and the current density may fluctuate over time. Therefore, in order to ensure reproducibility under the same conditions, more than three repeated experiments were performed for each condition.

The electrochemical properties of both mechanically polished and electropolished specimens were compared and analyzed using potentiodynamic polarization experiments in a PEMFC simulation solution. At this time, electropolishing was performed under conditions (electrolyte composition and potential) that produced the best surface quality. The PEMFC simulation solution recommended by the U.S. Department of Energy (DOE) was used, consisting of a pH 3 solution (H_2SO_4 + 0.1 ppm HF) at 80 °C [32,33]. The electrochemical experiments were conducted while continuously supplying oxygen gas to simulate the cathode environment. Additionally, to assess the changes in corrosion resistance due to electropolishing at the cathode, impedance spectroscopy was performed after 24 hours of immersion. The frequency range and amplitude were set to 100 kHz to 10 mHz and 10 mV, respectively.

2.2.3 Surface Analysis of Specimens

To analyze the phases and surface characteristics with electropolishing, an X-ray diffractometer (RIGAKU, SmartLab) was used. The 2θ range was set from 30° to 80°, and the scan was performed using Cu Kα radiation with a wavelength (λ) of 1.546 Å, a step size of 0.02° and a scan time of 1.0 second per step. Phase analysis was conducted by comparing the obtained XRD data with the ICDD database files. Surface analysis was performed using a stereomicroscope (OLYMPUSTM, SZX16), a 3D laser microscope (OLYMPUSTM, OLS5000LEXT), a field emission scanning electron microscope (FE-SEM, JEOL, JSM-7100) and energy-dispersive X-ray spectroscopy (EDS, OXPORD, AZTEc Energy).

3. Results and Discussion

3.1 Surface Treatment and Analysis

Fig. 1 presents the surface analysis results of titanium after mechanical polishing using a scanning electron

Table 2. Electrolyte compositions (Deep Eutectic Solvents, DES) for electropolishing at 35 °C

Unit	Level (molar ratio)		
Choline Chloride (ChCl), 99 %/w : Ethylene glycol (EG), 99 %/w	1 : 1	1 : 2	1 : 3

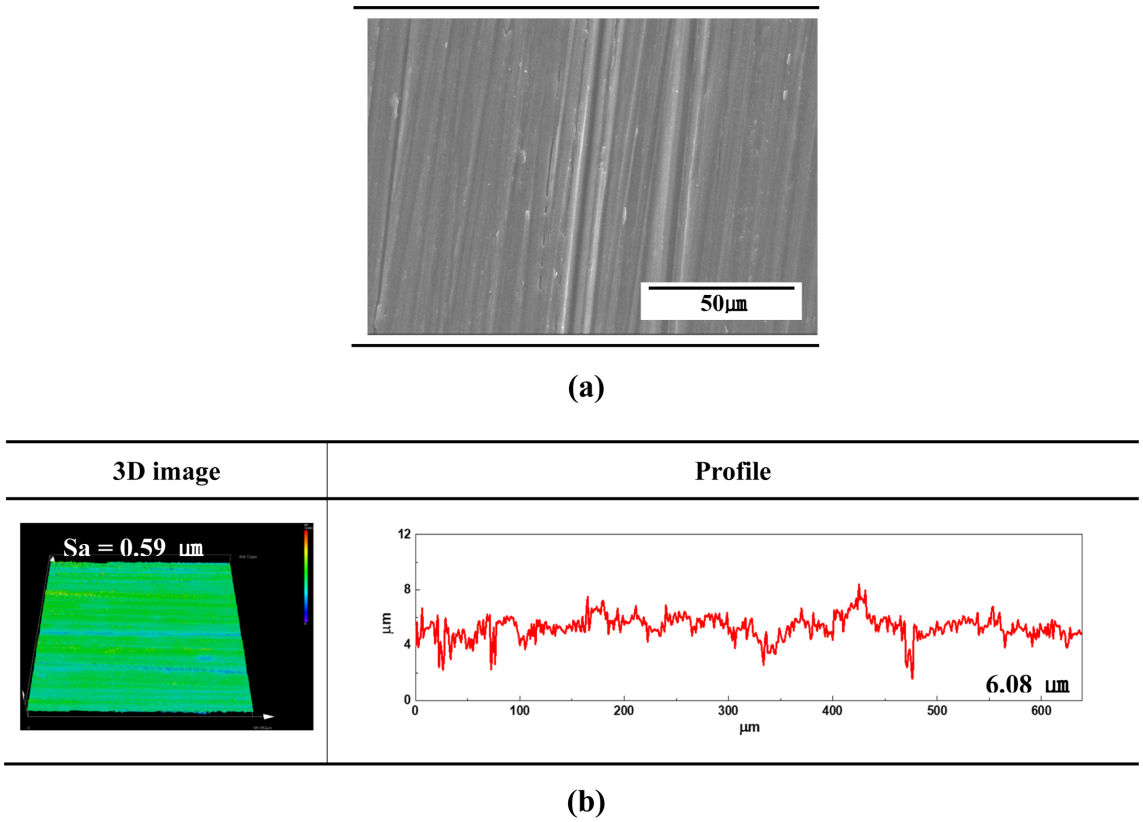

Fig. 1. SEM images (a), 3D image 2D profile (b) after mechanical polishing for titanium

microscope (a), 3D image and 2D profiling (b). The SEM observations revealed long, parallel grooves on the surface, formed in the direction of mechanical polishing. In industrial settings, high productivity often results in frequent occurrences of microdefects [34]. However, in this investigation, no microdefects were observed due to the controlled polishing process in a laboratory setting, including temperature control (cooling water supply) and speed regulation (inverter RPM control). The 2D profile analysis presented that the surface roughness and the height difference between peaks and valleys were 0.59 μm and 6.08 μm, respectively. Such irregular surfaces can negatively affect the quality of the coating layer, making additional pretreatment processes essential [35].

Fig. 2 presents the results of the potentiodynamic polarization experiment conducted in a mixed solution with a choline chloride to ethylene glycol ratio of 1:3. Electropolishing should be performed in a stable current density region within the passivation range identified in the polarization curves [36]. The purpose of electropolishing is to uniformly remove irregular peaks from the surface. In the passivation range, a thin oxide film forms on the metal surface, protecting it from rapid dissolution reactions. Also, the formation of this oxide layer stabilizes the dissolution rate, maintaining an overall balance. If electropolishing is performed outside this range, in either the transpassive or active regions, etching or pitting can occur on the metal surface [37]. This can lead to a roughened surface and the formation of microdefects, thereby compromising the quality of the electropolishing.

In the potentiodynamic polarization curve for the solution with a choline chloride to ethylene glycol ratio of 1:3, the delay in active dissolution was observed in two distinct regions. This suggests the presence of two passivation characteristics with different properties. In Fig. 2, it was observed that the current density remained constant at the relatively low potential ranges of 1.3 to 1.8 V and 2.4 to 2.7 V (vs Ag/AgCl). However, this current plateau range is not wide, ranging from approximately 0.3 to 0.5 V, so the passive film formed in this ranges is expected to be unstable. Accordingly, this range was not selected as a current plateau section. In the

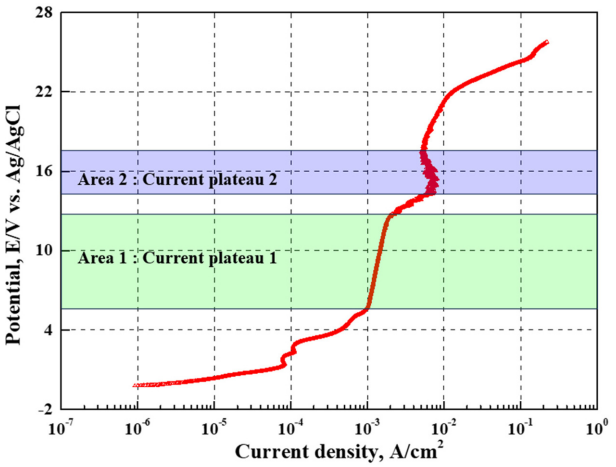

Fig. 2. Potentiodynimic polarization curve in a mixed solution of choline chloride and ethylene glycol in a ratio of 1:3

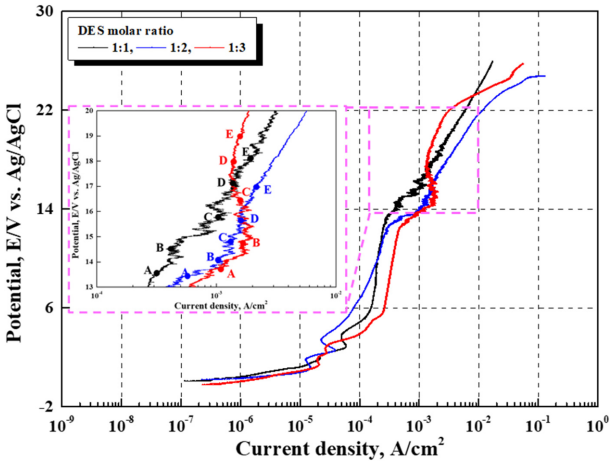

Fig. 3. Potentiodynamic polarization curves for titanium with DES composition A: Active potentials, B: Initial of plateau potentials, C: Middle of plateau potentials, D: End of plateau potentials, D: Transpassive potentials for electropolishing

first region, where a stable current density (current plateau) was formed at a lower potential, a thin oxide film formed on the surface, indicating passivation that delayed the dissolution reaction. The potential range for this region was observed to be between 5.76 V and 13.53 V.

In the second current plateau region at a higher potential, the oxide layer was considered to have thickened. This is thought to be the result of the formation of an additional oxide layer or a thicker oxide layer than the oxide layer formed at low potential. This higher energy provided the necessary driving force for the formation of the titanium oxide [20]. In particular, the driving force created by higher energy particularly provides more energy for ion movement through the oxide layer. Therefore, the titanium dioxide (TiO_2) layer formed at a higher potential may become denser and thicker than the layer formed at a lower potential. Additionally, at higher oxidation states, oxides such as TiO, Ti_3O_5 are likely to be formed [38].

Fig. 3 presents the results of the potentiodynamic polarization experiments conducted at 35 ºC in ethaline solutions with varying molar ratios of ethylene glycol. The polarization curves illustrate the electrochemical behavior of titanium as a function of current density and potential in ethaline. Electropolishing was primarily carried out in the second plateau region at higher potentials. This was done at a relatively low temperature of 35 ºC to ensure the safety of the polishing operator. At lower temperatures and potentials, insufficient energy is supplied to remove the oxide film and irregular valleys on titanium, which can significantly reduce the quality of the electropolishing.

Electropolishing was performed in five regions (A, B, C, D, E) including the second plateau region. Region A corresponds to the potential at which the titanium surface begins to dissolve. Region B marks the initial point of the plateau region where the passive film begins to form. Region C is the central part of the plateau region, where stable passivation characteristics are exhibited. Region D is the end of the plateau region, where the passive film is still present. Region E is where the passive film is disrupted or where oxygen evolution occurs, leading to an increase in current density.

The molar concentration of ethylene glycol affected the current density values within the plateau region, the stable current density range (B-D) and the potentials for pitting and oxygen evolution. This indicates that the ethylene glycol content influences the stability of the passive oxide film. As the ethylene glycol content increased, the current density in the initial stage of the plateau region (A-B) also increased. This suggests an acceleration of the ionization reaction. As a result, when the ethylene glycol molar ratio was highest (1:3), ionization reactions occurred more vigorously in the initial stage. Consequently, a thicker oxide layer was formed, leading to the most stable current density within the plateau region. The thickened oxide layer caused a gradual decrease in current density (B-D) as the potential increased within the plateau region.

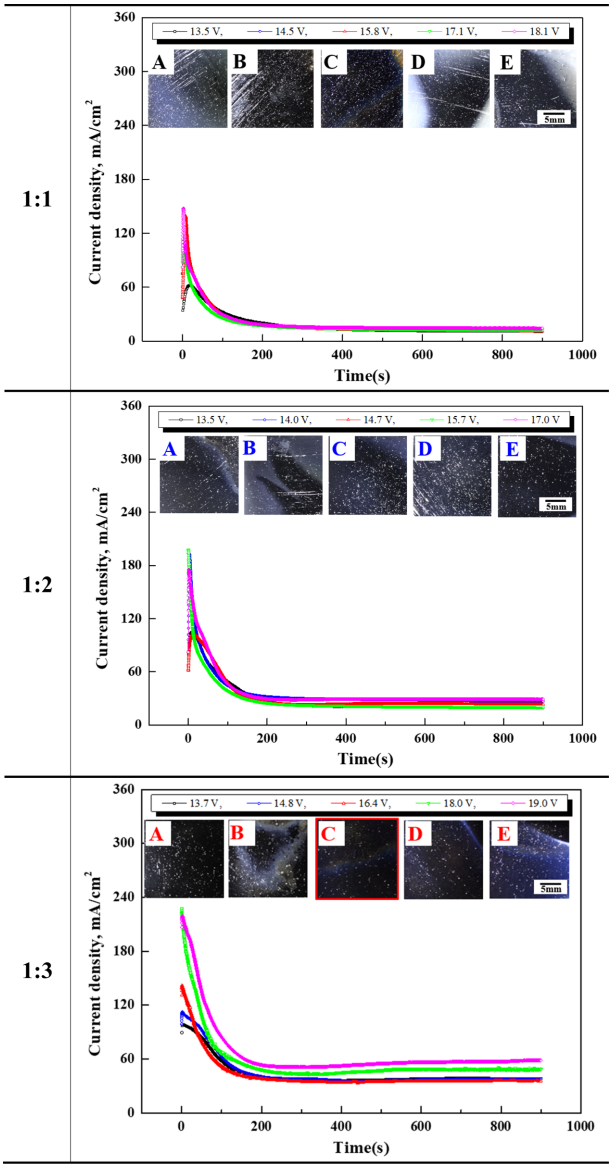

Fig. 4. Time - current density curve and appearance after electroplishing with DES composition for titanium

Fig. 4 exhibits the current density variation curve over time during electropolishing and the surface observation results after polishing. In this investigation, the current density initially increased rapidly before stabilizing, similar to other researches [39,40]. As the ethylene glycol content and voltage increased, the peak value of the initial current density also increased. As ethylene glycol reacts with titanium ions, forming a complex with hydrogen ions, an oxide film is generated, as shown in equation (1) [26].

$$Ti^{2+} + 2HOC_2H_4OH \rightarrow Ti(OC_2H_4OH)_2 + 2H^+ \quad (1)$$

$Ti(OC_2H_4OH)_2$ is an oxygen-bonded metal-organic complex that forms a stabilized protective film on the titanium surface and effectively controls the dissolution reaction. It also promotes the uniform growth of the oxide film in the electrolyte. As the ethylene glycol content increased, the concentration of active ions participating in the electrochemical reaction also increased, leading to a higher initial current density peak. Furthermore, higher voltages enhance the energy required to initiate electrochemical reactions. This results in more titanium being oxidized on the metal surface, accelerating the ionization reaction and increasing the initial current density. As time progresses, the complex formed on the surface controls the electrochemical reaction, leading to stable current density. Consequently, at 16.4 V in the ethaline solution with a 1:3 molar ratio of choline chloride to ethylene glycol, the smoothest surface was observed. A. Kityk *et al.* conducted cyclic voltammetry experiments to investigate the electrochemical behavior of titanium in ethaline, a deep eutectic solvent [26]. Their examination observed the first and second peaks in the cyclic voltammetry curves, the stable current region between the peaks attributed to the formation of complexes between titanium and ethylene glycol. Similarly, in this investigation, the stabilization trend of the current density after the first peak is considered to be due to the effective control of the dissolution reaction by the surface complexes.

Fig. 5 presents the 2D and 3D images, surface profiles and the height differences between peaks and valleys after electropolishing under various conditions. When the molar ratio of choline chloride to ethylene glycol was 1:1, the height difference between peaks and valleys gradually decreased as the potential increased. At relatively low potentials, the oxide film was thin and unevenly formed, leading to localized damage from the oxidation reaction. However, as the potential increased, the oxide film grew more stably, reducing the size of the surface damage and leading to a smoother surface. In the case of a 1:2 molar ratio of choline chloride to ethylene glycol, the height difference between peaks and valleys decreased as the potential increased from 13.5 V (A) to 14.7 V (C). This trend was similar to that observed with the 1:1 ratio. However, beyond this, localized damage increased, leading to a greater height difference between peaks and

	Potential	2D	3D	Profile	Height
1:1	A. 13.5 V		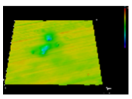	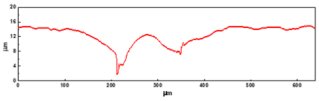	12.84 μm
	B. 14.5 V	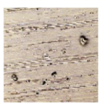	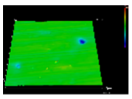	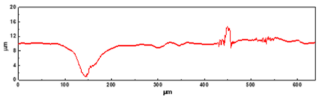	10.14 μm
	C. 15.8 V		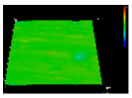	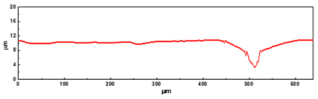	7.43 μm
	D. 17.1 V		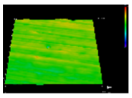	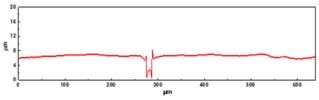	6.63 μm
	E. 18.1 V		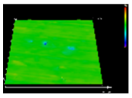	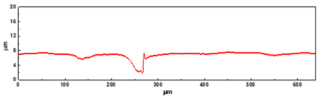	5.60 μm
1:2	A. 13.5 V	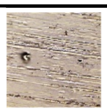	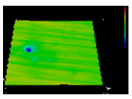	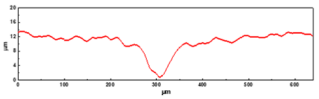	12.38 μm
	B. 14.0 V		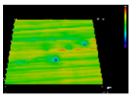	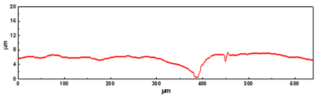	7.34 μm
	C. 14.7 V		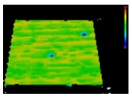	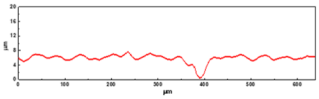	7.07 μm
	D. 15.7 V		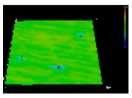	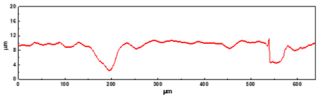	8.64 μm
	E. 17.0 V		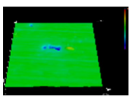	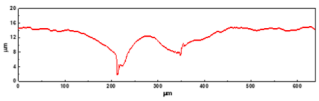	10.23 μm
1:3	A. 13.7 V	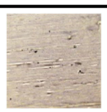	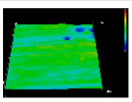	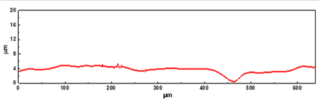	4.78 μm
	B. 14.8 V		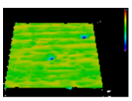	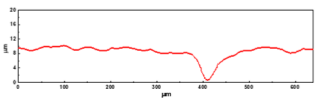	9.57 μm
	C. 16.4 V	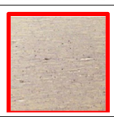	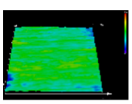	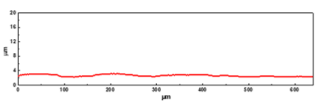	0.91 μm
	E. 18.0 V				4.10 μm
	D. 19.0 V				7.38 μm

Fig. 5. 2D, 3D image and height between mountain and valley after electropolishing with DES composition for titanium

valleys. In solutions with high ethylene glycol content, applying high voltage caused the oxide film to thicken, but it grew unevenly, leading to excessive localized oxidation reactions [41]. When the choline chloride to ethylene glycol ratio was 1:3, at 13.7 V (A) and 14.8 V (B), the oxide film formed was thin and uneven, similar to the 1:1 and 1:2 ratios. This resulted in relatively large height differences between peaks and valleys. However, at 16.4 V (C), the electropolishing effect was optimal, with a smooth, high-quality surface observed without any surface damage. At this potential, the oxide film exhibited optimal thickness and uniformity, maximizing the surface flattening effect. At 19.0 V (E), similar to the 1:2 ratio, excessive localized oxidation occurred, increasing the height difference between peaks and valleys on the surface.

Fig. 6 presents the surface observations after electropolishing at various potentials and ethylene glycol ratios using a field emission scanning electron microscope (FE-SEM). When the choline chloride to ethylene glycol ratios were 1:1 and 1:2, slight surface damage was observed. In contrast, with a choline chloride to ethylene glycol ratio of 1:3, the surface appeared smooth and flat without any damage. The damage observed at the 1:1 and 1:2 ratios can be explained as follows [22]. Initially, the substrate exhibits a thin passive layer when exposed to air. However, during electropolishing, the initially formed passive layer is removed, and a chloride layer is generated

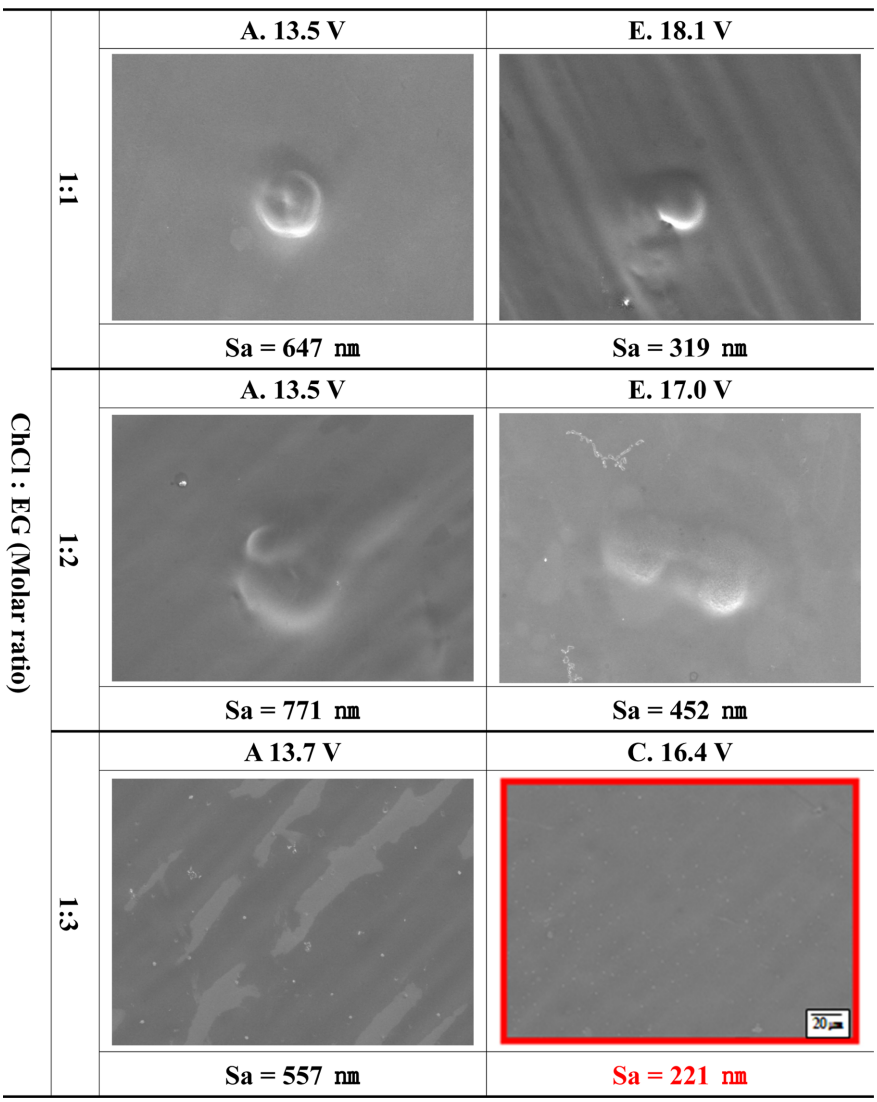

Fig. 6. Surface morphology and roughness after electropolishing with DES composition for titanium

by equation (2) [22].

$$TiO_2 + 4Cl^- + 4H^+ \rightarrow TiCl_4 + 2H_2O \quad (2)$$

The passive film dissolves due to the chloride ions, leading to localized corrosion where the surface is not uniformly ionized. However, as the ratio of choline chloride to ethylene glycol increased from 1:1 to 1:2, localized corrosion gradually decreased, and at a 1:3 ratio, no damage was observed. This indicates that the surface became more uniformly polished as the ethylene glycol ratio increased. Ethylene glycol, being a highly viscous solution, affects the mobility of ions, reducing the dissolution rate due to the ionization reaction of the metal [42]. Additionally, in a high-viscosity solution, the current density is more uniformly distributed, leading to a smoother surface. Consequently, the ratio of ethylene glycol plays a critical role in electrpolishing.

Fig. 7 compares the surface roughness (a) and the height difference between peaks and valleys (b) after electropolishing. In this investigation, the conditions with the lowest surface roughness and the smallest height difference between peaks and valleys were selected as the optimal conditions for electropolishing. The conditions with the lowest values in both surface roughness and height difference graphs—three to four conditions—were highlighted with red dotted lines. For surface roughness (a), the smallest values were observed in the C, D and A conditions with a 1:3 choline chloride to ethylene glycol ratio. Regarding the height difference between peaks and valleys (b), the smallest value was observed at condition C with a 1:3 choline chloride to ethylene glycol ratio, followed by conditions E, C and D with a 1:1 ratio. The difference in trends between surface roughness and height difference is attributed to localized corrosion caused by the chloride ions in the electrolyte [43]. If there is deep damage on an otherwise smooth surface, the surface roughness may be low, but the height difference between peaks and valleys can be significant. Ultimately, the conditions with the smallest surface roughness and height difference were the same, with the optimal electropolishing condition being C with a 1:3 choline chloride to ethylene glycol ratio. The detailed conditions are presented in Table 3.

Fig. 8 exhibits the XRD analysis results of titanium

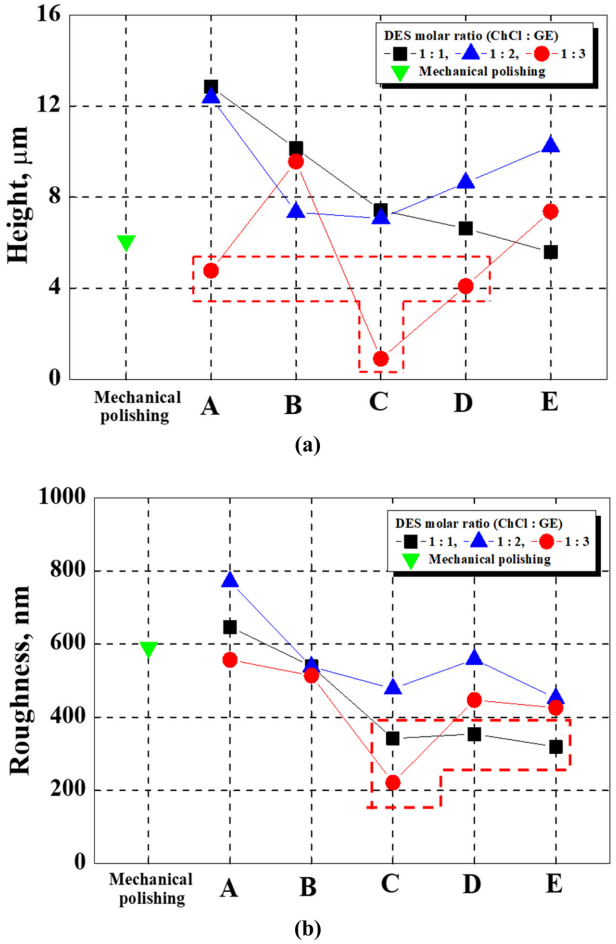

Fig. 7. Height (a) and roughness (b) comparison graph after electropolishing with DES composition for titanium

Table 3. Optimal conditions for electropolishing of titanium

Electrolyte composition (molar ratio)	Voltage	Temperature	Process time
ChCl : EG = 1 : 3	16.4 V	35 °C	15 minutes

after mechanical polishing and electropolishing under the optimal conditions. After mechanical polishing, titanium crystallinity was confirmed at diffraction angles of 36.09°, 38.42°, 40.12°, 53.05°, 62.93°, 70.62° and 76.19°. After electropolishing under optimal conditions, TiO_2 diffraction peaks were observed around 53.1°, 70.8° and 76.2°, which were confirmed to correspond to the (211), (301) and (420) planes of the rutile phase (JCPDS-ICDD 2003 file number 89-4920) [44]. Ruile phase TiO_2 has a denser crystal density and lower surface energy than the anatase and brookite phases, resulting in greater thermal and chemical stability. Accordingly, it is expected to

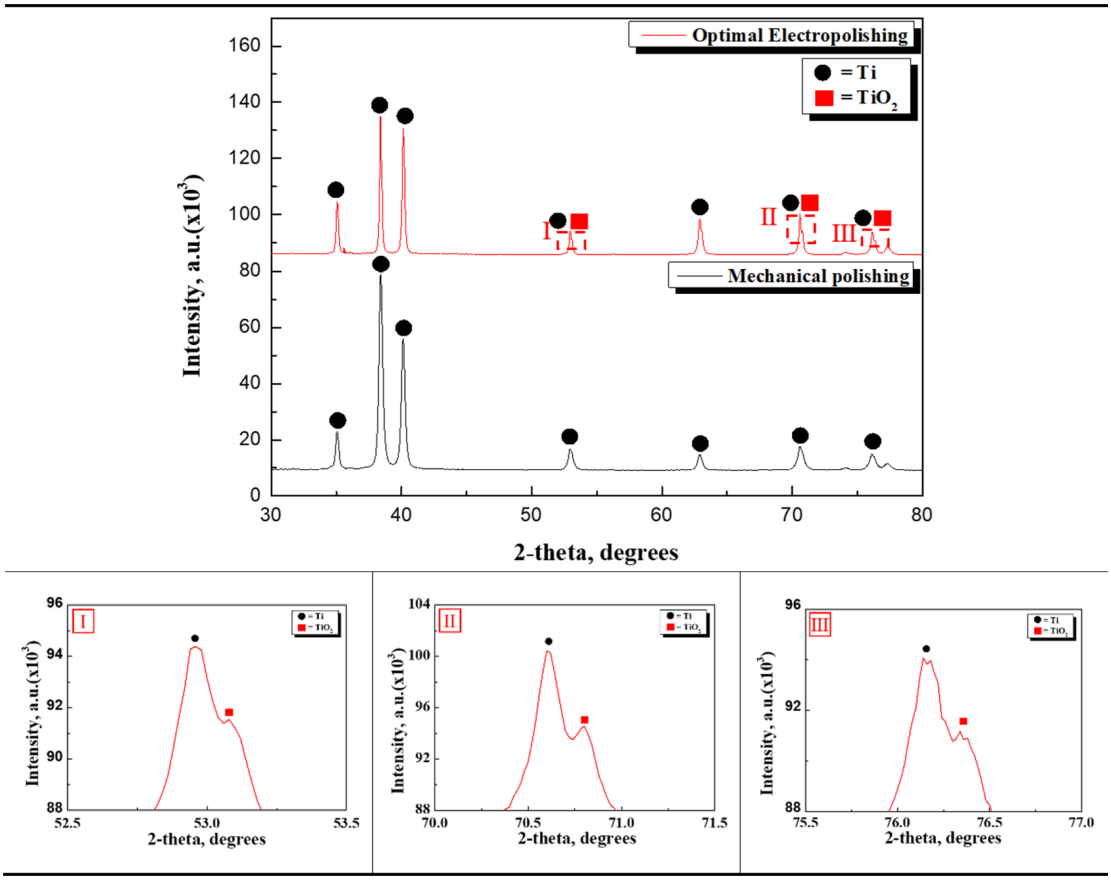

Fig. 8. XRD analysis with mechanical polishing and optimal electropolishing

exhibit excellent corrosion resistance in acidic environments such as PEMFC. The formation of this oxide layer on titanium polished under optimal conditions can be explained as follows [22]. Mechanical polishing flattens the surface using physical force, but the presence of contaminants generated during the polishing process can hinder the growth of the oxide layer. As a result, a sufficiently thick titanium dioxide layer to be detected by XRD was not formed. In contrast, during electropolishing under optimal conditions, the chloride layer formed as per equation (2) is eventually regenerated into an oxide layer by equation (3).

$$TiCl_4 + 2H_2O \rightarrow TiO_2 + 4HCl \quad (3)$$

The oxide layer could form thicker and more uniformly due to the applied potential exhibiting passive characteristics. Thus, the titanium dioxide generated by electropolishing was thick enough to be detected by XRD.

3.2 Electrochemical Experiments

Fig. 9 shows the potentiodynamic polarization experiment results in a PEMFC simulation solution under oxygen cathode conditions on titanium that was mechanically polished and electropolished under optimal conditions. The corrosion potential (E_{corr}) and corrosion current density (I_{corr}) of mechanically polished titanium were found to be -345.81 mV and 1.76 μA/cm^2, respectively. For titanium electropolished under optimal conditions, the corrosion potential and corrosion current density were observed to be -208.01 mV and 0.11 μA/cm^2, respectively. After electropolishing under optimal conditions, the corrosion potential increased by 39.85%, and the corrosion current density decreased by 93.75%. The pitting potential was found to be 1.28 V for mechanically polished titanium and 3.99 V for titanium electropolished under optimal conditions, indicating an increase of 2.71 V after electropolishing. When electropolishing was performed under optimal conditions, the corrosion resistance and pitting resistance were improved, resulting in the

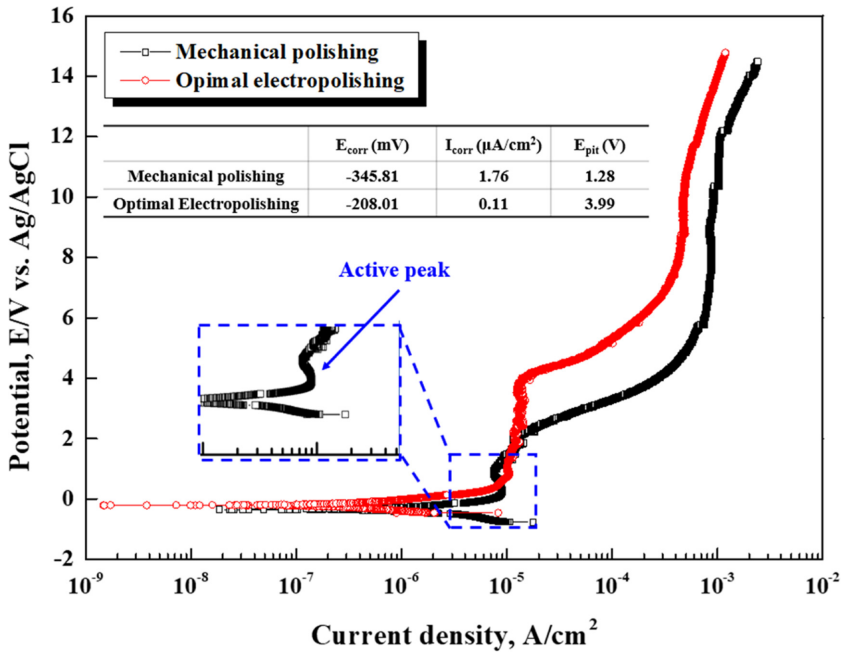

Fig. 9. Results obtained after potentiodynamic polarization experiments in DOE solution with mechanical polishing and optimal electropolishing

formation of a dense and uniform oxide film on the surface.

The U.S. Department of Energy (DOE) technical targets for the oxygen cathode require a corrosion current density below 1 $\mu A/cm^2$ and the absence of an active peak due to anodic dissolution [32,33]. Mechanically polished titanium did not meet the DOE standards, as the corrosion current density exceeded 1 $\mu A/cm^2$ and exhibited an active peak. In contrast, titanium polished under optimal conditions met the DOE standards, with a corrosion current density of 0.11 $\mu A/cm^2$ and no active peak observed. Thus, electropolishing was found to be a positive factor for application in PEMFC bipolar plates.

Fig. 10 exhibits the surface observation results after potentiodynamic polarization experiment on titanium with mechanical polishing and electropolishing under optimal conditions, using scanning electron microscopy and EDS analysis. For the specimens mechanically polished and electropolished under optimal conditions, the titanium content inside the damaged area was reduced compared to the outside. And the oxygen content was found to have increased compared to the outside. This suggests that an oxide layer was formed on the outer surface. However, in the titanium electropolished under optimal conditions, the oxygen content within the oxide layer was higher than in the mechanically polished specimen. This indicates that the oxide formed under optimal electropolishing conditions is denser, thicker and more uniform. Y. Zhang conducted a study on the effects of electropolishing on titanium alloys [45]. XPS analysis presented that in titanium alloys exposed to air, metallic titanium (453.66 eV, $Ti2p_{3/2}$) was observed, but after electropolishing, only the binding energy corresponding to TiO_2(458.64 eV) was detected. Similarly, in this investigation, it is inferred that TiO_2 formed more densely after optimal electropolishing, resulting in increased oxygen content.

In both mechanically polished and electropolished specimens, the oxide layer formed on the surface appears to have been damaged by the hydrogen ions and fluoride ions present in the electrolyte. Generally, the oxide layer is composed of titanium dioxide, and degradation occurs with equation (4) [46].

$$TiO_2 + 4H^+ + 6F^- \rightarrow TiF_6^{2-} + 2H_2O \quad (4)$$

The oxide layer on the electropolished specimen was denser and more uniform than on the mechanically polished one, resulting in narrower damaged areas compared to mechanical polishing. Finally, the surface

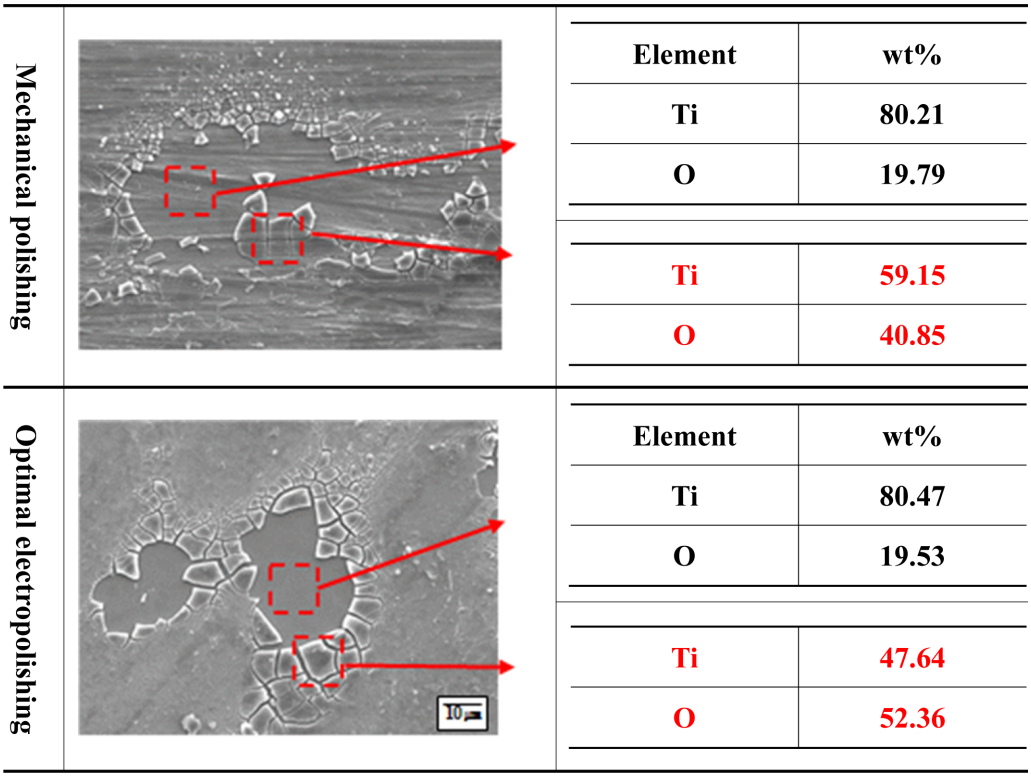

Element	wt%
Ti	80.21
O	19.79

Ti	59.15
O	40.85

Element	wt%
Ti	80.47
O	19.53

Ti	47.64
O	52.36

Fig. 10. SEM and EDS analysis after potentiodynamic polarization experiment in DOE solution with mechanical polishing and optimal electropolishing

damage observed was due to delamination caused by cracks in the oxide layer, rather than pitting-type localized corrosion. These shapes are thought to be due to the damage mechanism shown in Fig. 11 [47].

Fig. 11 illustrates the damage mechanism of the oxide layer on titanium mechanically polished and electropolished under optimal conditions with the potentiodynamic polarization experiment in the PEMFC simulation solution. Stage I represents the oxide layer formed on the titanium substrate. Based on EDS analysis and damage morphology observations in et al., the damage in both mechanically polished and optimal electropolished titanium appeared as delamination of the oxide layer. The higher oxygen content in the delaminated layer compared to the damaged interior indicates that the layer is indeed an oxide layer. The initial oxide layer is thin and stable on the substrate, providing excellent corrosion resistance. The outer environment contains oxygen and fluoride ions from the solution. In stage II, stress develops within the oxide layer, causing deformation. This stress likely results from differential expansion between the oxide layer and the substrate due to their different coefficients of expansion [48]. The oxide layer and substrate exhibit different thermal and electrochemical expansion characteristics. As heat and potential are applied, the oxide layer expands or contracts differently from the substrate, leading to internal stress. In stage III, fluoride ions in the solution selectively attack the oxide layer, thinning it locally, which further intensifies stress concentration. These factors complexly cause the oxide layer to delaminate from the substrate through a blistering effect. In stage IV, continued stress accumulation in the oxide layer eventually leads to crack formation, allowing oxygen from the solution to reach the substrate surface, where a new thin oxide layer forms. This new oxide layer, depicted in light blue in the schematic, corresponds to the approximately 19% oxygen content observed inside the delaminated damaged area in the EDS analysis in Fig. 10. In stage V, extensive cracking of the oxide layer occurs, leading to its eventual delamination. At this point, the extensive cracks allow more oxygen to penetrate, leading to the regeneration of a stable oxide layer. In stage

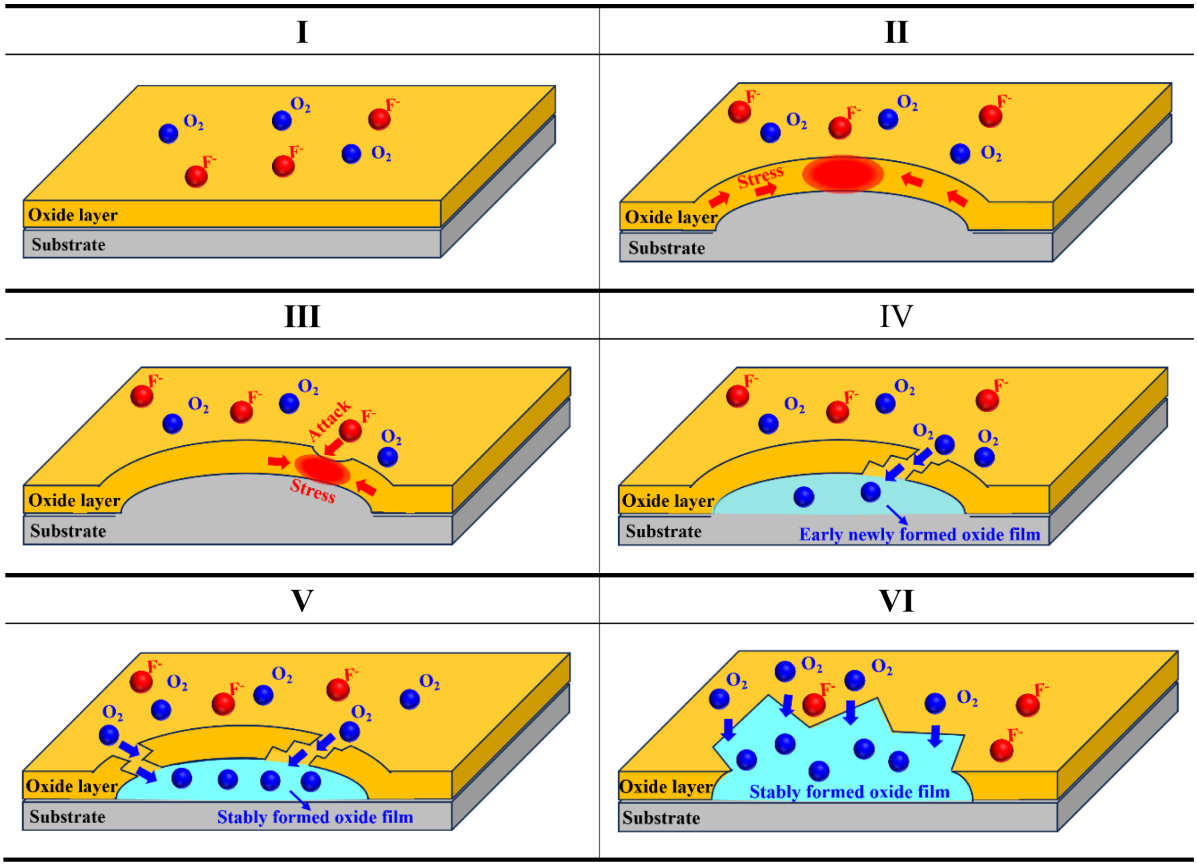

Fig. 11. Damage mechanism of titanium oxide layers with potentiodynamic polarization experiments in DOE solutions with mechanical polishing and optimal electropolishing

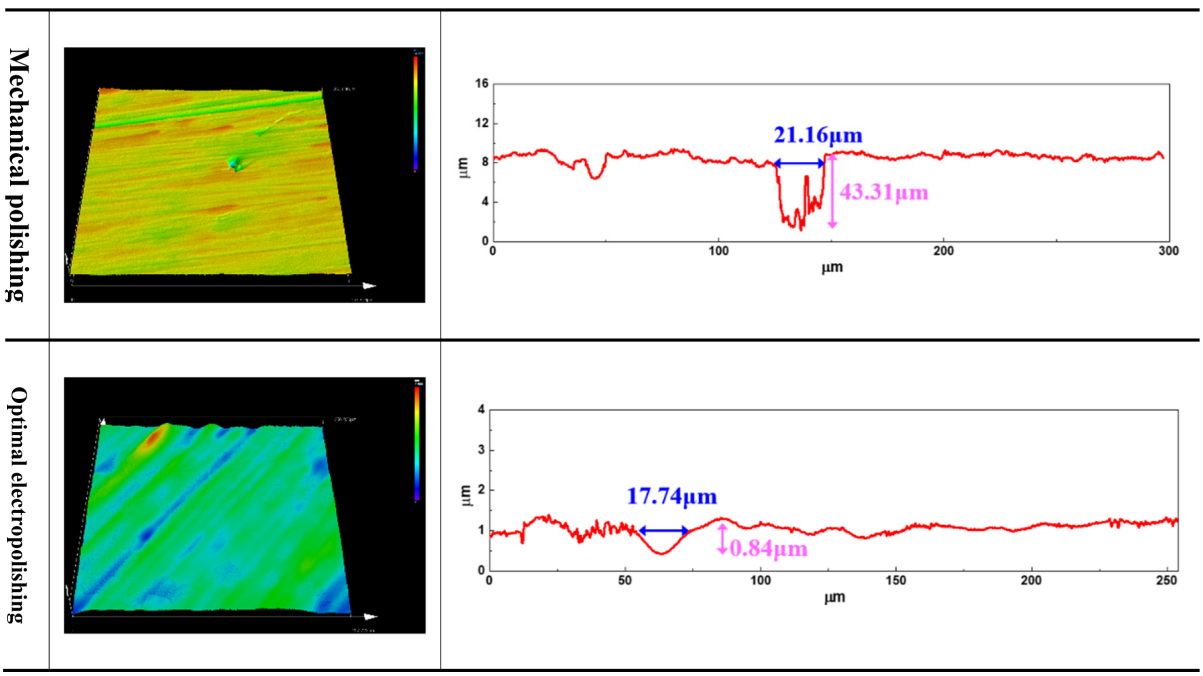

Fig. 12. 3D image and profile after potentiodynamic polarization experiment in DOE solution with mechanical polishing and optimal electropolishing

VI, the previously formed oxide layer delaminates, and a new oxide layer forms stably on the substrate.

Fig. 12 presents the 3D images and 2D profile analysis of the surface after potentiodynamic polarization experiment on titanium subjected to mechanical polishing and optimal electrochpolishing. For the mechanically polished specimen, the damage width and depth were measured to be 21.16 μm and 43.31 μm, respectively, while for the electropolished specimen, these values were 17.74 ㎛ and 0.84 μm, respectively. After electropolishing, the damage width and depth were reduced by 18.9% and 98.06%, respectively, compared to mechanical polishing. The difference in damage depth was more pronounced than that in damage width. Y. C. Wu *et al.* investigated the electrochemical behavior of rough surfaces in Ti6Al4V produced by electron beam melting additive manufacturing, which were flattened by electropolishing [48]. Their research reported that in electropolished specimens, as surface roughness decreased, uneven features such as grooves and gaps were reduced. As a result, a uniform oxide film formed on the surface, inhibiting corrosion reactions [48]. In this examination as well, the lower surface roughness of electropolished specimens at optimal condition likely contributed to the formation of a uniform oxide film, reducing localized damage.

Fig. 13 exhibits the Nyquist plot (a), Bode impedance plot (b), Bode phase angle plot (c) and equivalent circuit (d) obtained after 24 hours of immersion in a PEMFC simulation solution under oxygen cathode conditions for mechanically polished and optimal electropolished titanium. In the Nyquist plot, a larger semicircle radius indicates a higher impedance real value at the same imaginary part, representing greater resistance to charge

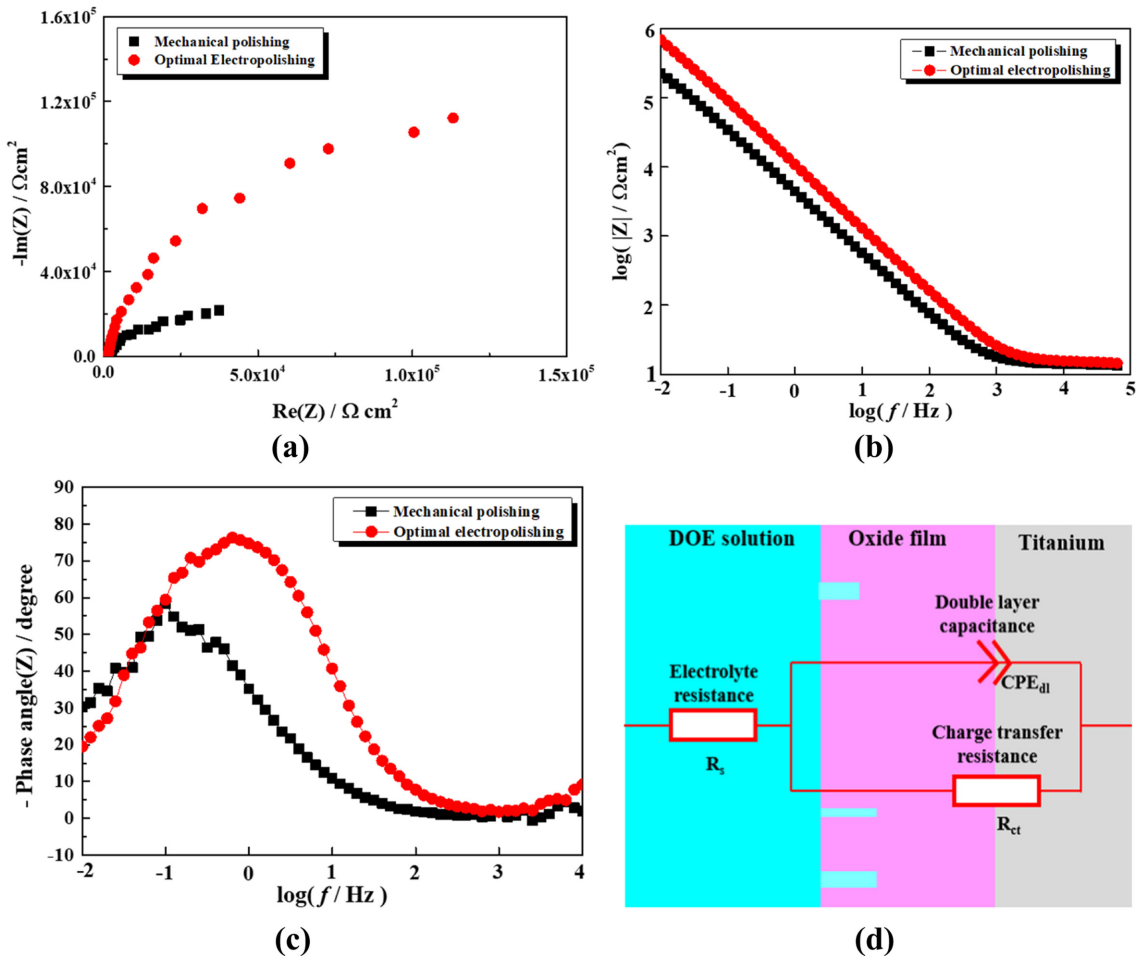

Fig. 13. Nyquist plot(a), bode plots(b, c), equivalent circuit(d) by electrochemical impedance spectroscopy after immersion in a DOE solution for 24 hours with mechanical polishing and optimal electropolishing

transfer [49]. Thus, the increased charge transfer resistance after electropolishing indicates improved corrosion resistance.

In the Bode impedance plot (b), the electropolished specimen exhibited higher impedance modulus | Z | (Y-axis) across all frequency ranges (X-axis) compared to the mechanically polished specimen. This suggests that the oxide layer formed by electropolishing acts as a dense barrier, inhibiting corrosion.

In the Bode phase angle plot (c), the phase angle (Y-axis) of the electropolished specimen was observed to be higher than that of the mechanically polished specimen. A higher phase angle indicates capacitor-like behavior on the surface, suggesting a superior ability to store charge [50].

Consequently, the oxide layer formed after electropolishing is stable and dense, capable of effectively storing charge. Thus, the equivalent circuit of titanium can be represented as shown in (d). R_s and R_{ct} represent the resistance of the electrolyte and charge transfer, respectively, and CPE_{dl} represents the capacitance of the electrical double layer. Since the electrical double layer in the passive film of general metals is not ideal, it is represented by CPE_{dl}. Therefore, the oxide layer provides resistance to charge transfer, which correlates with the enhanced corrosion resistance.

The electropolished flat surface is advantageous in improving adhesion force and ensuring uniform deposition thickness when forming hard thin films such as TiN, TiC and TiCN, which are physical vapor deposition-based coatings. In particular, the electropolished surface has no pores and low surface roughness, significantly reducing the possibility of pinhole or void formation during sputtering or arc deposition. Accordingly, it is expected that this will contribute to improving the corrosion resistance and electrical conductivity of metallic bipolar plates for PEMFCs. In addition, when sol-gel-based carbon is coated on a TiO_2-based surface formed by electropolishing, the electron transfer path is expected to be expanded, thereby improving the interfacial electron transfer characteristics between the coating layer and the base material.

4. Conclusion

The investigation on the effects of electropolishing using choline chloride-based deep eutectic solvents with varying ethylene glycol molar ratios (1:1, 1:2, 1:3) and applied potentials, as well as the electrochemical characteristics in a PEMFC simulated environment, yielded the following results:

1. The ethylene glycol molar ratio affected the current density values, the stability of the current density plateau, the pitting and oxygen evolution potentials in the plateau region. As the concentration of ethylene glycol increased, the current density in the current plateau region remained the most stable.
2. Surface observations after electropolishing revealed that at 16.4 V (the central potential within the current plateau range) with a 1:3 choline chloride to ethylene glycol ratio, the surface was smooth and undamaged, indicating a high-quality electropolishing effect. Under this condition, the oxide film exhibited optimal thickness and uniformity, maximizing the surface flattening effect.
3. After electropolishing under optimal conditions, the corrosion current density decreased by 93.75% compared to mechanical polishing, and the pitting potential increased by 2.71 V. This indicates that corrosion resistance and pitting resistance were significantly improved after electropolishing.
4. The corrosion current density of titanium polished under optimal conditions was found to be below 1 μA/cm^2, with no active peak observed, meeting the U.S. Department of Energy standards.
5. Surface morphology observations after potentiodynamic polarization experiment on titanium subjected to mechanical polishing and optimal electropolishing revealed that the surface exhibited delamination due to blistering of the oxide layer, rather than pitting-type localized corrosion.

Acknowledgments

This research was supported by National University Development Project through the National Research Foundation of Korea funded by the Ministry of Education.

References

1. B. S. Fromm, B. L. Adams, S. Ahmadi, M. Knezevic, Grain size and orientation distributions: application to

yielding of α-titanium, *Acta Materialia*, **57**, 2339 (2009). Doi: https://doi.org/10.1016/j.actamat.2008.12.037
2. G. Lütjering, J. C. Williams, Titanium Matrix Composites, In: Titanium. Engineering Materials and Processes, pp. 313 – 328, Springer, Berlin, Heidelberg (2003). Doi: https://doi.org/10.1007/978-3-540-71398-2_9
3. Y. J. Choi, C. Y. Jeong, Nano-engineering of Hybrid Titanium Oxide Structure (TiO_2) using Pore-widening Concentration for Enhanced Superhydrophilicity, *Corrosion Science and Technology*, **23**, 41 (2024). Doi: https://doi.org/10.14773/CST.2024.23.1.41
4. A. A. Ahmed, A. Y. Burjes, M. Z. Elias, Effects of pH and Chloride Concentration on Corrosion Behavior of Duplex Stainless Steel and Titanium Alloys Ti 6Al 2Nb 1Ta 1Mo at Elevated Temperature for Pump Impeller Applications, *Corrosion Science and Technology*, **21**, 454 (2022). Doi: https://doi.org/10.14773/CST.2022.21.6.454
5. N. C. Ferreri, Daniel J. Savage, Marko Knezevic, Non-acid, alcohol-based electropolishing enables high-quality electron backscatter diffraction characterization of titanium and its alloys: Application to pure Ti and Ti-6Al-4V, *Materials Characterization*, **166**, 110406, (2020). Doi: https://doi.org/10.1016/j.matchar.2020.110406
6. T. Fast, M. Knezevic, S.R. Kalidindi, Application of microstructure sensitive design to structural components produced from hexagonal polycrystalline metals, *Computational Materials Science*, **43**, 374 (2008). Doi: https://doi.org/10.1016/j.commatsci.2007.12.002
7. N. Landry, M. Knezevic, Delineation of first-order elastic property closures for hexagonal metals using fast Fourier transforms, *Materials*, **8**, 6326 (2015). Doi: https://doi.org/10.3390/ma8095303
8. Y. S. Tian, C. Z. Chen, S. T. Li, Q. H. Huo, Research progress on laser surface modification of titanium alloys, *Applied Surface Science*, **242**, 177 (2005). Doi: https://doi.org/10.1016/j.apsusc.2004.08.011
9. N. F. Asri, T. Husaini, A. B. Sulong, E. H. Majlan, W. R. W. Daud, Coating of stainless steel and titanium bipolar plates for anticorrosion in PEMFC: A review, *International Journal of Hydrogen Energy*, **42**, 9135 (2017). Doi: https://doi.org/10.1016/j.ijhydene.2016.06.241
10. Z. Xu, Z. Li, R. Zhang, T. Jiang, L. Peng, Fabrication of micro channels for titanium PEMFC bipolar plates by multistage forming process, *International Journal of Hydrogen Energy*, **46**, 11092 (2021). Doi: https://doi.org/10.1016/j.ijhydene.2020.07.230
11. E. A. Bel'skaya, An experimental investigation of the electrical resistivity of titanium in the temperature range from 77 to 1600 K, *High Temperature*, **43**, 546 (2005). Doi: https://doi.org/10.1007/s10740-005-0096-2
12. J. Matolich Jr, Thermal conductivity and electrical resistiv-ity of type 316 stainless steel from 0 to 1800f (No. NASA-CR-54151) (1965). https://ntrs.nasa.gov/api/citations/19650024830/downloads/19650024830.pdf
13. P. Yi, W. Zhang, F. Bi, L. Peng, X. Lai, Enhanced corrosion resistance and interfacial conductivity of TiC x/a-C nanolayered coatings via synergy of substrate bias voltage for bipolar plates applications in PEMFCs, *ACS Applied Materials & Interfaces*, **10**, 19087 (2018). Doi: https://doi.org/10.1021/acsami.8b00514
14. D. H. Shin, S. J. Kim, Effects of Thickness and Defects of DLC Coating Layer on Corrosion Resistance of Metallic Bipolar Plates of PEMFCs, *Corrosion Science and Technology*, **23**, 235 (2024). Doi: https://doi.org/10.14773/cst.2024.23.3.235
15. D. H. Shin, S. J. Kim, Effects of Temperature and Chloride Concentration on Electrochemical Characteristics and Damage Behavior of 316L Stainless Steel for PEMFC Metallic Bipolar Plate, *Corrosion Science and Technology*, **21**, 300 (2022). Doi: https://doi.org/10.14773/cst.2022.21.4.300
16. R. Xu, X. Jin, H. Bi, Z. Zhang, and M. Li, Effect of surface roughness on contact resistance and electrochemical corrosion behavior of 446 stainless steel in simulated anode environments for proton exchange membrane fuel cell, *Journal of Solid State Electrochemistry*, **28**, 3087 (2024). Doi: https://doi.org/10.1007/s10008-024-05864-z
17. Q. Hu, D. Zhang, H. Fu, K. Huang,Investigation of stamping process of metallic bipolar plates in PEM fuel cell—Numerical simulation and experiments, *International Journal of Hydrogen Energy*, **39**, 13770(2014). Doi: https://doi.org/10.1016/j.ijhydene.2014.01.201
18. R. Ryszard, T. Hryniewicz, Enhanced oxidation-dissolution theory of electropolishing, *Transactions of the IMF*, **90**, 188 (2012). Doi: https://doi.org/10.1179/0020296712Z.00000000031
19. J. Y. Jang, J. S, Song, and J. S. Nah, Effect of polishing solution temperature and times by electro-polishing in dental casting Co-Cr-Mo alloy, *Journal of Technologic Dentistry*, **34**, 145 (2012). Doi: https://doi.org/10.14347/kadt.2012.34.2.145
20. D. Landolt, Fundamental aspects of electropolishing, *Electrochimica Acta*, **32**, 11 (1987). Doi: https://doi.org/10.1016/0013-4686(87)87001-9

21. W. O. Karim, A. P. Abbott, S. Cihangir, K. S. Ryder, Electropolishing of nickel and cobalt in deep eutectic solvents, *Transaction of the IMF*, **96**, 200 (2018). Doi: https://doi.org/10.1080/00202967.2018.1470400
22. D. h. Kim, K. S. Son, D. H. Sung, Y. H. Kim, W. S. Chung, Effect of added ethanol in ethylene glycol–NaCl electrolyte on titanium electropolishing, *Corrosion Science*, **98**, 494 (2015). Doi: https://doi.org/10.1016/j.corsci.2015.05.057
23. X. SUN, X. WEI, Z. LI, D. LOU, Y. WANG, H. LIU, Experimental Investigation of Electropolishing in Ethylene Glycol-NaCl Electrolyte for Surface Integrity of Nitinol Cardiovascular Stents, *Electrochemistry*, **88**, 325 (2020). Doi: https://doi.org/10.5796/electrochemistry.20-00047
24. C. Rotty, A. Mandroyan, M. L. Doche, S. Monney, J. Y. Hihn, N. Rouge, Electrochemical superfinishing of cast and ALM 316L stainless steels in deep eutectic solvents: surface microroughness evolution and corrosion resistance, *Journal of The Electrochemical Society*, **166**, C648 (2019). Doi: https://doi.org/10.1149/2.1211913jes
25. A. Kityk, M. Hnatko, V. Pavlik, M. Boča, Electrochemical surface treatment of manganese stainless steel using several types of deep eutectic solvents, *Materials Research Bulletin*, **141**, 111348 (2021). Doi: https://doi.org/10.1016/j.materresbull.2021.111348
26. A. Kityk, V. Protsenko, F. Danilov, V. Pavlik, M. Hnatko, J. Šoltýs, Enhancement of the surface characteristics of Ti-based biomedical alloy by electropolishing in environmentally friendly deep eutectic solvent (ethaline), *Colloids and Surfaces A: Physicochemical and Engineering Aspects*, **613**, 126125 (2021). Doi: https://doi.org/10.1016/j.colsurfa.2020.126125
27. S. T. Hwang, S. H. Cheon, J. S. Song, Y. H. Yun, B. H. Kim, X. Zhang, D. U. Kim, D. S. Hyun, B. S. Oh, A Study to Improve PEMFC Performance by Using Electro Polishing and CrN Coating on Metal Bipolar Plate, *Transactions of the Korean Society of Automotive Engineers*, **22**, 65 (2014). Doi: https://doi.org/10.7467/ksae.2014.22.4.065
28. L. Casanova, M. Gruarin, M. Pedeferri, M. Ormellese, A comparison between corrosion performances of titanium grade 2 and 7 in strong reducing acids, *Materials and Corrosion*, **72**, 1506 (2021). Doi: https://doi.org/10.1002/maco.202112392
29. R. Schenk, The Corrosion Properties of Titanium and Titanium Alloys, In: Titanium in Medicine. Engineering Materials. Springer, Berlin, Heidelberg (2001). Doi: https://doi.org/10.1007/978-3-642-56486-4_6
30. A. Kityk, M. Hnatko, V. Pavlik, M. Boča, Electrochemical surface treatment of manganese stainless steel using several types of deep eutectic solvents, *Materials Research Bulletin*, **141**, 111348 (2021). Doi: https://doi.org/10.1016/j.materresbull.2021.111348
31. M. J. Choi, E. B. Jo, D. J. Kim, Optimal Electropolishing Condition of Austenitic Stainless Steel Specimens for Slow Strain Rate Tensile Testing, *Corrosion Science and Technology*, **22**, 457 (2023). Doi: https://doi.org/10.14773/CST.2023.22.6.457
32. W. S. Yang, J. H. Lee, H. S. Roh, J. H. Yoo, C. M. Park, S. Y. Lee, S. M. Moon, Comparison Study of Polymer and Ti Sol-Gel Carbon Coating on Ti for PEMFC Bipolar Plates, *Corrosion Science and Technology*, **22**, 447 (2023) Doi: https://doi.org/10.14773/CST.2023.22.6.447
33. H. S. Heo, S. J. Kim, Electrochemical Characteristics of MMO(Ti/Ru)-Coated Titanium in a Cathode Environment of Polymer Electrolyte Membrane Fuel Cell MMO(Ti/Ru), *Corrosion Science and Technology*, **21**, 340 (2022) Doi: https://doi.org/10.14773/CST.2022.21.5.340
34. Hua Wang, Defects tracking in mass customisation production using defects tracking matrix combined with principal component analysis, *International Journal of Production Research*, **51**, 1852 (2012). Doi: https://doi.org/10.1080/00207543.2012.718449
35. P. Panjan, P. Gselman, D. Kek-Merl, M. Čekada, M. Panjan, G. Dražić, T. Bončina, F. Zupanič, Growth defect density in PVD hard coatings prepared by different deposition techniques, *Surface and Coatings Technology*, **237**, 349 (2013). Doi: https://doi.org/10.1016/j.surfcoat.2013.09.020
36. Shuo-Jen Lee, Yi-Ho Chen, Jung-Chou Hung, The Investigation of Surface Morphology Forming Mechanisms in Electropolishing Process, *International Journal of Electrochemical Science*, **7**, 12495 (2012). Do: https://doi.org/10.1016/S1452-3981(23)16561-8
37. S. Zaki, N. Zhang, M. D. Gilchrist, Electropolishing and Shaping of Micro-Scale Metallic Features, *Micromachines*, **13**, 468 (2022). Doi: https://doi.org/10.3390/mi13030468
38. T. Leichtweiss, R. A. Henning, J. Koettgen, R. M. Schmidt, B. Holländer, M. Martin, M. Wuttig, J. Janek, Amorphous and highly nonstoichiometric titania (TiOx) thin films close to metal-like conductivity, *Journal of Materials Chemistry A*, **2**, 6631 (2014). Doi: https://doi.org/10.1039/C3TA14816E

39. H. K. Hwang, S. J. Kim, Electrochemical characteristics and damage mechanism in scrubber washing water of UNS N08367 with plasma ion nitriding and electropolishing, *npj Materials Degradation*, **8**, 1 (2024). Doi: https://doi.org/10.1038/s41529-024-00474-6
40. Rong Yi, Jianwei Ji, Zejin Zhan, Hui Deng, Mechanism study of electropolishing from the perspective of etching isotropy, *Journal of Materials Processing Technology*, **305**, 117599 (2022). Doi: https://doi.org/10.1016/j.jmatprotec.2022.117599
41. Y. Kang, S. Yan, Z. Li, Z. Wang, A. Yang, W. Ma, W. Chen, Y. Qu, Influence of Anodic Oxidation on the Organizational Structure and Corrosion Resistance of Oxide Film on AZ31B Magnesium Alloy, *Coatings*, **14**, 271 (2024). Doi: https://doi.org/10.3390/coatings14030271
42. A. M. Awad, N. A. Abdel Ghany, T. M. Dahy, Removal of tarnishing and roughness of copper surface by electropolishing treatment, *Applied Surface Science*, **256**, 4370 (2010). Doi: https://doi.org/10.1016/j.apsusc.2010.02.033
43. J. S. Lee, S. W. Park Effect of Phosphate Surface Treatment on the Localized Corrosion Resistance of UNS G41400 Steel, UNS G41400, *Corrosion Science and Technology*, **22**, 429 (2023). Doi: https://doi.org/10.14773/CST.2023.22.6.429
44. Morad, M. M. El-Desoky, A. Mansour, M. Wasfy, Synthesis, structural and electrical properties of PVA/TiO_2nanocomposite films with different TiO_2 phases prepared by sol-gel technique, *Journal of Materials Science: Materials in Electronics*, **27**, 17574 (2020). Doi: https://doi.org/10.1007/s10854-020-04313-7
45. Y. Zhang, J. Li, S. Che, Y. Tian, Electrochemical Polishing of Additively Manufactured Ti–6Al–4V Alloy, *Metals and Materials International*, **26**, 783 (2020). Doi: https://doi.org/10.1007/s12540-019-00556-0
46. J. Shi, P. Zhang, Y. Han, H. Wang, X. Wang, Y. Yu, J. Sun, Investigation on electrochemical behavior and surface conductivity of titanium carbide modified Ti bipolar plate of PEMFC, *International Journal of Hydrogen Energy*, **45**, 10050 (2020). Doi: https://doi.org/10.1016/j.ijhydene.2020.01.203
47. A. S. Ulrich, U. Glatzel, & M. C. Galetz, Discontinuities in Oxidation Kinetics: A New Model and its Application to Cr–Si-Base Alloys, *Oxidation of Metals*, **95**, 445 (2021). Doi: https://doi.org/10.1007/s11085-021-10029-8
48. Y. C. Wu, C. N. Kuo, Y. C. Chung, C. H. Ng, J. C. Huang, Effects of Electropolishing on Mechanical Properties and Bio-Corrosion of Ti6Al4V Fabricated by Electron Beam Melting Additive Manufacturing, *Materials*, **12**, 1466 (2019). Doi: https://doi.org/10.3390/ma12091466
49. H. Luo, C. F. Dong, X. G. Li, K. Xiao, The electrochemical behaviour of 2205 duplex stainless steel in alkaline solutions with different pH in the presence of chloride, *Electrochimica Acta*, **64**, 211 (2012). Doi: https://doi.org/10.1016/j.electacta.2012.01.025
50. C. Q. Ye, R. G. Hu, S. G. Dong, X. J. Zhang, R, Q, Hou, R. G. Du, C. J. Lin, and J. S. Pan, EIS analysis on chloride-induced corrosion behavior of reinforcement steel in simulated carbonated concrete pore soultions, *Journal of Electroanalytical Chemistry*, **688**, 275 (2013). Doi: https://doi.org/10.1016/j.jelechem.2012.09.012